

DM-Align: Leveraging the Power of Natural Language Instructions to Make Changes to Images

Maria Mihaela Trusca¹, Tinne Tuytelaars², Marie-Francine Moens¹

¹KU Leuven, Department of Computer Science

²KU Leuven, Department of Electrical Engineering

{mariamihaela.trusca, tinne.tuytelaars, sien.moens}@kuleuven.be

Abstract

Text-based semantic image editing assumes the manipulation of an image using a natural language instruction. Although recent works are capable of generating creative and qualitative images, the problem is still mostly approached as a black box sensitive to generating unexpected outputs. Therefore, we propose a novel model to enhance the text-based control of an image editor by explicitly reasoning about which parts of the image to alter or preserve. It relies on word alignments between a description of the original source image and the instruction that reflects the needed updates, and the input image. The proposed Diffusion Masking with word Alignments (DM-Align) allows the editing of an image in a transparent and explainable way. It is evaluated on a subset of the Bison dataset and a self-defined dataset dubbed Dream. When comparing to state-of-the-art baselines, quantitative and qualitative results show that DM-Align has superior performance in image editing conditioned on language instructions, well preserves the background of the image and can better cope with long text instructions.

1 Introduction

AI-driven image generation was confirmed as a smooth-running option for content creators with high rates of efficiency and also creativity (Ramesh et al., 2022) that can be easily adapted to generate consecutive frames for video generation (Ding et al., 2022; Singer et al., 2023). Text-based guidance has proven to be a natural and effective means of altering visual content in images. Various model architectures have been proposed for text-based image synthesis, ranging from transformers (Ding et al., 2021; Vaswani et al., 2017) to generative adversarial networks (GANs) (Goodfellow et al., 2014; Reed et al., 2016; Zhu et al., 2019), and more recently, diffusion models like DALL-E 2 (Ramesh et al., 2022), Imagen (Saharia et al., 2022), or Stable Diffusion Models (Rombach et al., 2022). The

Source Caption: A photo of a **British shorthair cat** wearing a **cowboy hat** and **red shirt** skateboarding.
Target Caption: A photo of a **Shiba Inu dog** wearing a **cowboy hat** and **red shirt** skateboarding.

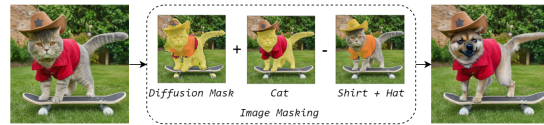


Figure 1: The proposed image editor utilizes a source caption to describe the initial image and a target text instruction to define the desired edited image. To accomplish this task, we employ the two captions to generate a diffusion mask, refining it further by incorporating regions of words that we want to keep or alter in the image.

success of diffusion models, akin to that observed in language models (Kaplan et al., 2020), largely results from their scalability. Factors such as model size, training dataset size, and computational resources contribute significantly to their effectiveness, overshadowing the impact of the model architecture itself. This scalability enables these models to adapt easily to different domains, including unseen concepts (Ramesh et al.; Saharia et al., 2022). Moreover, these models are ready to use without the need for additional training (Choi et al., 2021; Li et al., 2020).

While similar to the text-based semantic image generation task in its creation of new visual content, text-guided image editing also relies on additional visual guidance. Consequently, the goal of text-guided image manipulation is to modify the content of a picture according to a given text while keeping the remaining visual content untouched. The remaining visual content is from now on referred to as “background”. As text-to-image generators, text-based image editors work at the frame level and can be further adapted for video editing (Zhang et al., 2023b). Text-based semantic image editing typically employs text-based image generation models with user-defined image masks (Avrahami et al., 2023, 2022; Wang et al., 2023; Xie et al., 2023).

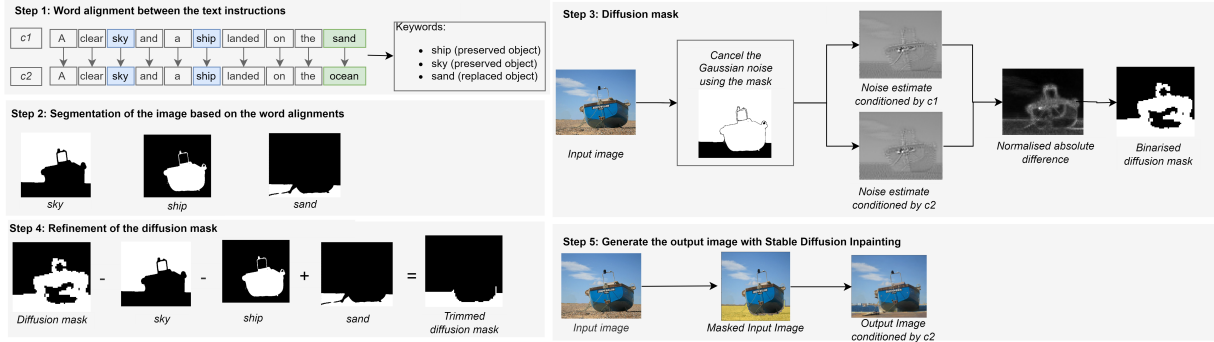


Figure 2: The implementation of DM-Align. The aim is to update the input image described by the text instruction c_1 (“A clear sky and a ship landed on the sand”) according to the text instruction c_2 (“A clear sky and a ship landed on the ocean”).

Each of these masks is an arrangement that differentiates between the image content that is to be changed or preserved. However, asking humans to generate masks is cumbersome, so we would like to edit images naturally, relying solely on a textual description of the image and its instruction to change it. Existing models for text-based semantic image editing, which do not require human-drafted image masks, struggle to maintain the background (Brooks et al., 2023; Couairon et al., 2022; Kawar et al., 2023; Tumanyan et al., 2023; Zhang et al., 2023a). Preserving the background’s consistency is particularly relevant for applications like game development or virtual worlds, where visual continuity across frames is crucial. Finally, the complexity of textual instructions given by their length poses a challenge for semantic image editors. While the existing models can effectively handle short text instructions, they encounter difficulties in manipulating an image using longer and more elaborate ones.

To address the aforementioned limitations, we present a novel approach that employs one-to-one alignments between the words in the text instruction describing the source image and those describing the desired edited image (Figure 1). By leveraging these word alignments, we implement image editing as a series of deletion, insertion, and replacement operations. Through this text-based control mechanism, our proposed model consistently produces high-quality editing results, even with long text instructions, while ensuring the preservation of the background.

As presented in Figure 2, we align the words of the text that describes the source image and the textual instruction that describes how the image should look after the editing, which allows us to

determine the information the user wants to keep, or replace. Then, disjoint regions associated with the preserved or discarded information are detected by segmenting the image. Next, a global, rough mask for inpainting is generated using standard diffusion models. While the diffusion mask allows the insertion of new objects that are larger than the replaced ones, it has the disadvantage of being too rough. Therefore, we further refine it using again the detected disjoint regions. To prove the effectiveness of DM-Align, the masked content is generated using inpainting stable diffusion (Rombach et al., 2022).

Our contributions are summarized as follows:

1. Our novel approach reasons with the text caption of the original input image and the text instruction that guides the changes in the image, which is a natural and human-like way of approaching image editing with a high level of explainability.
2. By differentiating between the image content to be changed from the content to be left unaltered, the proposed DM-Align enhances the text control of semantic image editing.
3. Compared to recent models for text-based semantic image editing, DM-Align demonstrates superior capability in handling long text instructions and preserving the background of the input image while accurately implementing the specified edits.

2 Related work

Despite the aim of keeping the background as similar as possible to the input image, numerous AI-based semantic image editors insert unwanted alter-

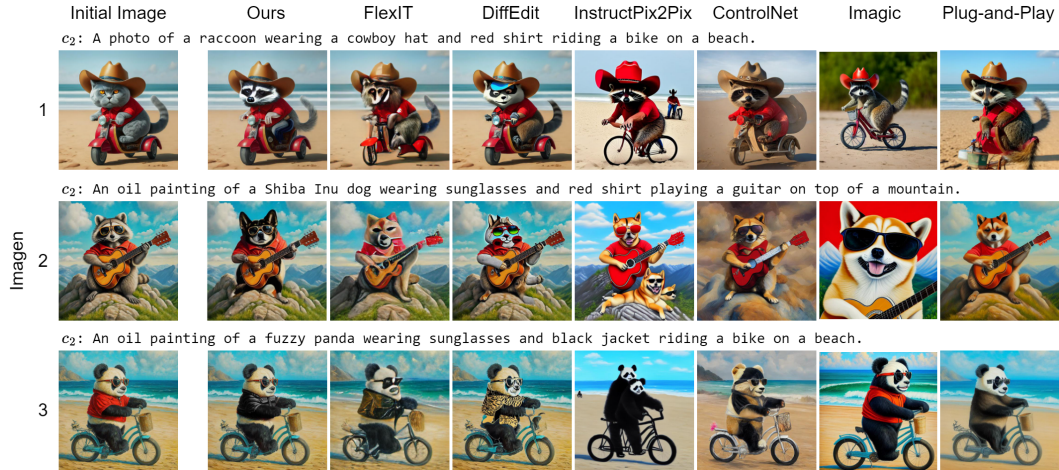


Figure 3: Semantic image editing: Imagen dataset. Source captions: (1) c_1 . A photo of a British shorthair cat wearing a cowboy hat and red shirt riding a bike on a beach. (2) c_1 . An oil painting of a raccoon wearing sunglasses and red shirt playing a guitar on top of a mountain. (3) c_1 . An oil painting of a fuzzy panda wearing sunglasses and red shirt riding a bike on a beach.

ations in the image. FlexIt (Couairon et al., 2022) combines the input image and instruction text into a single target point in the CLIP multimodal embedding space and iteratively transforms the input image toward this target point. Zhang et al. (2023a) introduce ControlNet as a neural network based on two diffusion models, one frozen and one trainable. While the trainable model is optimized to inject the textual conditionality of the semantic editing, the frozen model preserves the weights of the model pre-trained on large image corpora. The output of ControlNet is gathered by summing the outputs of the two diffusion models. To keep the structural information of the input image, Tumanyan et al. (2023) define a Plug-and-Play model as a variation of the Latent Diffusion Model. Their method edits an input image using not only textual guidance but also a set of features that separately store spatial information and layout details like the shape of objects.

While most text-based image editors are training-free, Imagic proposed by Kwar et al. (2023), assumes fine-tuning of the diffusion model by iteratively running over a text embedding optimized to match the input image and resemble the editing text instruction. Ultimately, the text embedding of the editing instructions and the optimized text embedding are interpolated and utilized as input by the fine-tuned model to generate the final edited image. This idea of fine-tuning a diffusion model is also adopted by Brooks et al. (2023) to define InstructPix2Pix as a model that approaches text-based image editing as a supervised task. Due

to the scarcity of data, a methodology relying on Prompt-to-Prompt (Hertz et al., 2023) is proposed for generating pairs of images before and after the update. During inference, the fine-tuned stable diffusion model can seamlessly edit images using an input image and a text instruction.

The above approaches lack an explicit delineation of the image content to be altered. Closer to our work is the Prompt-to-Prompt model (Hertz et al., 2023) which connects the text prompt with different image regions using cross-attention maps. The image editing is then performed in the latent representations responsible for the generation of the images. In contrast, our work focuses on the detection and delineation of the content to be altered in the image and is guided by the difference in textual instructions. Additionally, we edit images using real pictures and not latent representations artificially generated by a source prompt.

To overcome the problem of unwanted alterations in the image, DiffEdit (Couairon et al., 2023) computes an image mask as the difference between the denoised outputs using the textual instruction that describes the source image and the instruction that describes the desired edits. However, without an explicit alignment between the two text instructions and the input image, DiffEdit has little control over the regions to be replaced or preserved. While DiffEdit internally creates the editing mask, models like SmartBrush (Xie et al., 2023), Imagen Editor (Wang et al., 2023), Blended Diffusion (Avrahami et al., 2022) or Blended Latent Diffusion (Avrahami et al., 2023) directly edit images

using hand-crafted user-defined masks.

Due to a rough text-based control, the above models often struggle with preserving background details and are overly sensitive to the length of text instructions. Different from the current models, our DM-Align model does not treat the recognition of the visual content that requires preservation or substitution as a black box. By explicitly capturing the semantic differences between the natural language instructions, DM-Align provides comprehensive control over image editing. This novel approach results in superior preservation of unaltered image content and more effective processing of long text instructions. Except for the models that require additional input masks, all the above-mentioned text-based image editors are used as baselines for our evaluation.

3 Proposed model

In this section, we present our solution for semantic image editing. We define the task and then describe the main steps of the proposed model, which consist of: 1) Detecting the content that needs to be updated or kept relying on the alignment of words of the text that describes the source image and the textual instruction that describes how the image should look after the editing; 2) The segmentation of the image content to be updated or kept by cross-modal grounding; 3) The computation of a global diffusion mask that assures the coherence of the updated image; 4) The refinement of the global diffusion mask with the segmented image content that will be updated or kept; and 5) The inpainting of the mask with the help of a diffusion model. As demonstrated by our experiments, the proposed DM-Align can successfully replace, delete, or insert objects in the input image according to the text instructions. Our method mainly focuses on the nouns of the text instructions and their modifiers. Consequently, DM-Align does not implement action changes and the resulting changes in the position or posture of objects in the input image, which we leave for future work.

3.1 Task Definition

DM-Align aims to alter a picture described by a source text description or instruction c_1 using a target text instruction c_2 . Considering this definition, the purpose is to adjust only the updated content mentioned in the text instruction c_2 and leave the remaining part of the image unchanged. Based on

this, we argue the need for a robust masking system that clearly distinguishes between unaltered image regions, which we call “background”, and the regions that require adjustments.

3.2 Word alignment between the text instructions

The alignment represents the first step of the DM-Align model proposed to enhance the text-based control for semantic image editing (Figure 2). Given the two text instructions c_1 and c_2 , our assumption is that the shared words should indicate unaltered regions, while the substituted words should point to the regions that require manipulations. Implicitly, the most relevant words for this analysis are nouns due to their quality of representing objects in the picture. The words are syntactically classified using the Stanford part-of-speech tagger (Toutanova et al., 2003).

We extend the region to be edited by including the regions of the shared words with different word modifiers¹ in the two text instructions. As a result, the properties of the already existing objects in the picture can be updated. On the contrary, if the aligned nouns have identical modifiers (or no modifiers) in both instructions, their regions in the image should be unaltered. In addition, we also consider the regions of the unaligned nouns mentioned in the source text instruction (deleted nouns) as unaltered regions. Keeping the regions of the deleted nouns is important because we assume that in the target instruction, a user only mentions the desired changes in the image, omitting irrelevant content (Hurley, 2014). Editing the regions of the deleted nouns reduces the similarity w.r.t the source image and increases the level of randomness in the target image since we generate new visual content that is irrelevant to both the source image and the target caption (Figure 11).

Considering the example presented in Figure 4, the diffusion mask is adjusted to include the regions assigned to the sofa and dress. While the sofa is substituted with a bench, the dress has different modifiers in the captions. On the other hand, the regions of nouns “girl” and “cat” are eliminated from the diffusion mask. The girl is mentioned in both captions, while the cat is irrelevant to the user according to the caption c_2 and is incorporated in

¹A modifier is a word or phrase that offers information about another word mentioned in the same sentence. To keep the editing process simple, in the current work we use only word modifiers represented by adjectives.

the background.

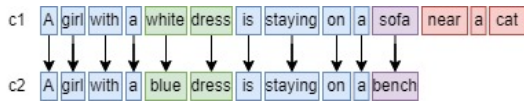


Figure 4: Word alignment example. Blue: identical words, Purple: substituted words, Green: nouns with different modifiers, Red: nouns mentioned only in the source caption c_1 .

The detection of word alignments between the two text instructions is realized with a neural semi-Markov CRF model (Lan et al., 2021). The model is trained to optimize the word span alignments, where the maximum length of spans is equal to D words (in our case $D = 3$). The obtained word span alignments will then further be refined into word alignments.

The neural semi-Markov CRF model is optimized to increase the similarity between the aligned source and target word span representations, which are each computed with a pretrained SpanBERT model (Joshi et al., 2020). The component that optimizes the similarity between these representations is implemented as a feed-forward neural network with Parametric ReLU (He et al., 2015). To avoid alignments that are far apart in the source and target instructions, another component controls the Markov transitions between adjacent alignment labels. To achieve this, it is trained to reduce the distance between the beginning index of the current target span and the end index of the target span aligned to the former source span. Finally, a Hamming distance is used to minimize the distance between the predicted alignment and the gold alignment. The outputs of the above components are fused in a final function $\psi(a|s,t)$ that computes the score of an alignment a given a source text s and target text t . The conditional probability of span alignment a is then computed as:

$$p(a|s,t) = \frac{e^{\psi(a|s,t)}}{\sum_{a' \in \mathcal{A}} e^{\psi(a'|s,t)}} \quad (1)$$

where the set \mathcal{A} denotes all possible span alignments between source text s and target text t . The model is trained by minimizing the negative log-likelihood of the gold alignment a^* from both directions, that is, source to target $s2t$ and target to source $t2s$:

$$\sum_{s,t,a^*} -\log p(a_{s2t}^*|s,t) - \log p(a_{t2s}^*|t,s) \quad (2)$$

The neural semi-Markov CRF model is trained on the MultiMWA-MTRef monolingual dataset, a subset of the MTReference dataset (Yao, 2014). Considering the trained model, we predict the word alignments as follows. Given two text instructions c_1 and c_2 , the model predicts two sets of span alignments a : a_{s2t} aligning c_1 to c_2 ; and a_{t2s} aligning c_2 to c_1 . The final word alignment is computed by merging these two span alignments. Let i be a word of the source text and j be a word of the target text, if alignment a_{s2t} indicates the connection $i \rightarrow j$ and alignment a_{t2s} indicates the connection $j \rightarrow i$, then the words i and j become aligned. In the end, the word alignments are represented by a set of pairs $(i - j)$, where i is a word of the instruction c_1 , and j is a word of the instruction c_2 .

3.3 Segmentation of the image based on the word alignments

The aim is to identify the regions in the image that require changes or conservation (second step in Figure 2). Based on the above word alignments, we select the nouns whose regions will be edited (non-identical aligned nouns or aligned nouns with different modifiers in the two text instructions) and the nouns whose regions will stay unaltered (nouns of the source text instruction not shared with the target text instruction, identical aligned nouns). Once these nouns are selected we use Grounded-SAM (Charles, 2023) to detect their corresponding image regions. Its benefit is the ‘‘open-set object detection’’ achieved by the object detector Grounding DINO (Liu et al., 2023) which allows the recognition of each object in an image that is mentioned in the language instruction. Given a noun, Grounding DINO detects its bounding box in the image, and SAM (Kirillov et al., 2023) determines the region of the object inside the bounding box. The selected regions will be used to locally refine the diffusion masks discussed in the next section.

3.4 Diffusion mask

To ensure the coherence of the complete image given the target language instruction and to cope with the cases when the object to be replaced is smaller than the object to be inserted, we also use a global diffusion mask. The computation of the diffusion mask represents the third step of our proposed model (Figure 2) and relies on the denoising diffusion probabilistic models (DDPM) (Ho et al., 2020; Weng, 2021). DDPMs are based on Markov chains that gradually convert the input data

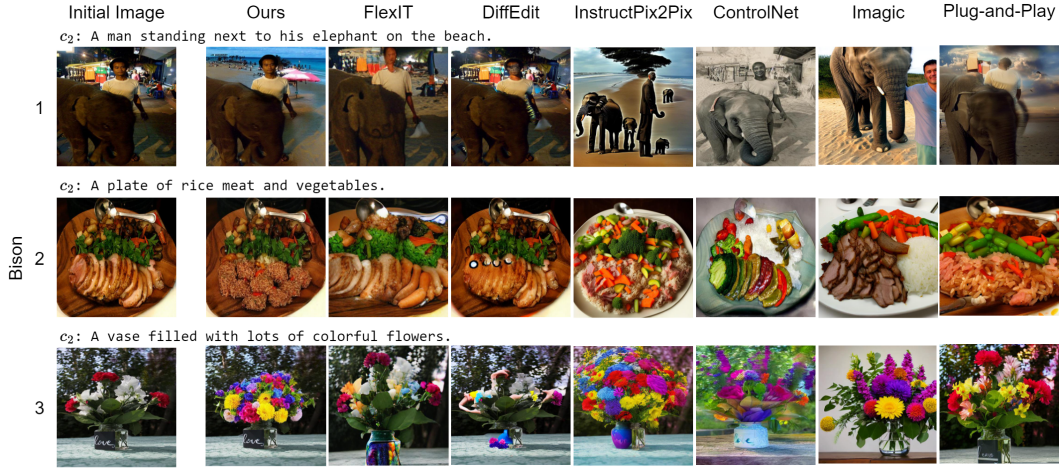


Figure 5: Semantic image editing: Bison dataset. Source captions: (1) c_1 . A man standing next to a baby elephant in the city. (2) c_1 . A wooden plate topped with sliced meat and vegetables. (3) c_1 . A vase filled with red and white flowers.

into Gaussian noise during a forward process, and slowly denoise the sampled data into newly desired data during a reverse process. In each iteration t of the forward process, new data x_t is sampled from the distribution $q(x_t|x_{t-1}) = \mathcal{N}(\sqrt{1-\beta_t}x_{t-1}, \beta_t I)$, where β_t is an increasing coefficient that varies between 0 and 1 and controls the level of noise for each time step t . The process is further simplified by expressing the sampled data x_t w.r.t the input image x_0 , as follows:

$$x_t = \sqrt{\alpha_t}x_0 + \sqrt{1-\alpha_t}\varepsilon \quad (3)$$

where $\alpha_t = \prod_{i=0}^t(1-\beta_i)$ and $\varepsilon \sim \mathcal{N}(0, 1)$ represents the noise variable. As we empirically observed that the editing effect is diminished over the regions where the noise variable is cancelled, we set the noise variable ε to 0 over the regions that should be preserved. We dubbed this operation noise cancellation. The forward process is executed for T iterations until x_T converges to $\mathcal{N}(0, 1)$. During the reverse process, at each time step $t-1$, x_{t-1} is denoised from the distribution $q_\theta(x_{t-1}|x_t)$ defined as:

$$q_\theta(x_{t-1}|x_t) = \mathcal{N}\left(\frac{1}{\sqrt{1-\beta_t}}(x_t - \frac{\beta_t}{\sqrt{1-\alpha_t}}\varepsilon_\theta(x_t)), \frac{1-\alpha_{t-1}}{1-\alpha_t}\beta_t\right) \quad (4)$$

where $\varepsilon_\theta(x_t, t)$ is estimated by a neural network usually represented by a U-Net.

To impose the text conditionally in a diffusion model, we have to integrate the text instruction c into the U-Net model and compute $\varepsilon_\theta(x_t|c)$, instead

of $\varepsilon_\theta(x_t)$. Using classifier-free guidance (Saharia et al., 2022) and knowing that s ($s > 1$) represents the guidance scale, $\varepsilon_\theta(x_t)$ mentioned in Eq. 4 is replaced by $\bar{\varepsilon}_\theta(x_t|c)$ defined as:

$$\bar{\varepsilon}_\theta(x_t|c) = s\varepsilon_\theta(x_t|c) + (1-s)(\varepsilon_\theta(x_t|0)) \quad (5)$$

To obtain the diffusion mask, we first compute the denoised output of the input image corresponding to the source instruction and the denoised output of the input image corresponding to the target instruction by running two separate DDPM processes. The diffusion process does not run over the input image but over its encoded representation yielded by a Variational Autoencoder (VAE) (Kingma and Welling, 2014; Rombach et al., 2022) with Kullback-Leibler loss. Therefore, the denoised outputs do not represent the final edited image but only an intermediate image representation with semantic information associated with the source or target instruction. Inspired by Couairon et al. (2023), we compute the diffusion mask as the absolute difference between the two noise estimates that is rescaled between $[0, 1]$ and binarized using a threshold set to 0.5. This diffusion mask represents a global mask that roughly indicates the content to be changed.

3.5 Refinement of the diffusion mask

The refinement of the diffusion mask represents the fourth step of DM-Align as presented in Figure 2. To further improve the precision of the global diffusion mask, we refine it using the regions detected in Section 3.3. More specifically, we extend the diffusion mask to include the regions to be altered and

Table 1: Image-level evaluation for Dream, Bison and Imagen datasets (mean and variance). Compared with the baselines, DM-Align achieves the best image-based scores while FlexIT obtains the best similarity w.r.t the target instruction as indicated by CLIPScore. Knowing that the CLIPScore is heavily biased for models based on the CLIP model (as FlexIT does), and considering the image-based scores, DM-Align achieves the best trade-off between similarities to the input image and the target instruction.

		FID↓	LPIPS↓	PWMSE↓	CLIPScore↑
Dream	FlexIT	150.20 ± 0.67	0.53 ± 0.00	47.63 ± 0.13	0.87 ± 0.00
	InstructPix2Pix	158.77 ± 3.03	0.44 ± 0.00	43.20 ± 0.44	0.81 ± 0.00
	ControlNet	140.42 ± 0.38	0.49 ± 0.00	49.6 ± 0.46	0.80 ± 0.00
	DiffEdit	126.77 ± 0.14	0.29 ± 0.57	30.22 ± 0.14	0.72 ± 0.00
	Plug-and-Play	128.13 ± 0.98	0.53 ± 0.00	48.56 ± 0.13	0.76 ± 0.00
	Imagic	157.06 ± 0.23	0.65 ± 0.00	48.23 ± 0.03	0.79 ± 0.00
	DM-Align	124.57 ± 0.52	0.31 ± 0.00	29.24 ± 0.03	0.80 ± 0.00
Bison	FlexIT	41.78 ± 0.09	0.50 ± 0.00	42.59 ± 0.03	0.90 ± 0.00
	InstructPix2Pix	62.62 ± 0.17	0.53 ± 0.00	41.45 ± 0.01	0.78 ± 0.00
	ControlNet	45.87 ± 0.38	0.45 ± 0.00	52.12 ± 0.11	0.78 ± 0.00
	DiffEdit	53.54 ± 0.22	0.45 ± 0.00	49.65 ± 0.18	0.76 ± 0.00
	Plug-and-Play	52.44 ± 0.18	0.46 ± 0.00	48.45 ± 0.15	0.76 ± 0.00
	Imagic	63.23 ± 0.28	0.52 ± 0.00	51.44 ± 0.12	0.77 ± 0.00
	DM-Align	40.05 ± 0.03	0.39 ± 0.00	37.05 ± 0.07	0.78 ± 0.00
Imagen	FlexIT	91.86 ± 0.32	0.46 ± 0.00	44.05 ± 0.00	0.91 ± 0.00
	InstructPix2Pix	133.33 ± 0.04	0.57 ± 0.00	42.68 ± 0.18	0.79 ± 0.00
	ControlNet	85.86 ± 0.26	0.51 ± 0.00	58.44 ± 0.04	0.79 ± 0.00
	DiffEdit	101.73 ± 0.00	0.38 ± 0.00	30.02 ± 0.09	0.71 ± 0.00
	Plug-and-Play	84.37 ± 0.29	0.41 ± 0.00	41.79 ± 0.07	0.78 ± 0.00
	Imagic	94.92 ± 0.44	0.67 ± 0.00	51.58 ± 0.11	0.77 ± 0.00
	DM-Align	66.68 ± 0.01	0.31 ± 0.00	29.04 ± 0.01	0.79 ± 0.00

Table 2: Image-level evaluation of DM-Align on a subset of the Bison dataset that contains only source and target text instructions with a degree of similarity higher than Rouge 0.7. Out of all baselines, only FlexIT and DiffEdit are presented, as they utilize a source caption in their implementation. While DM-Align scores better than the baselines for image-based metrics, FlexIT has the highest CLIPScore due to its CLIP-based architecture.

	FID↓	LPIPS↓	PWMSE↓	CLIPScore↑
FlexIT	71.64 ± 0.03	0.48 ± 0.00	42.30 ± 0.03	0.89 ± 0.00
DiffEdit	74.60 ± 0.94	0.44 ± 0.01	51.75 ± 0.29	0.76 ± 0.00
DM-align	67.91 ± 0.00	0.36 ± 0.00	36.28 ± 0.00	0.78 ± 0.00

shrink it to avoid editing over the preserved regions. To improve control over the preserved background, we adjust the noise variable over the forward process of the obtained diffusion mask. The noise variable is cancelled for the unaltered regions detected in the previous step and kept unchanged for the regions to be manipulated.

Note that both the global diffusion mask with noise cancellation and the regions determined through image segmentation are necessary for a qualitative mask. The global diffusion mask facilitates the replacement of small objects with larger ones and gives context to the editing. On the other hand, the insertion or deletion of different regions based on image segmentation improves the precision of the final mask as shown in ablation experiments in Subsection 5.1.

Once the refined diffusion mask is computed, we use inpainting stable diffusion (Rombach et al.,

2022) to edit the masked regions based on the given target text caption (fifth step of DM-Align presented in Figure 2). We also tried to replace the inpainting stable diffusion with latent blended diffusion (Avrahami et al., 2023). However, the obtained results were slightly worse, and the computational time increased by 60% (details are in Table 6 of Appendix C).

4 Experimental setup

Baselines. We compare results obtained with DM-Align with those of FlexIT (Couairon et al., 2022), DiffEdit (Couairon et al., 2023), ControlNet (Zhang et al., 2023a), Plug-and-Play (Brooks et al., 2023), Imagic (Kawar et al., 2023) and InstructPix2Pix (Tumanyan et al., 2023). The implementation details are presented in Appendix A.

Datasets. While ControlNet, Plug-and-Play, Imagic and InstructPix2Pix are evaluated on

Table 3: Background-level evaluation for Dream, Imagen and Bison datasets (mean and variance). DM-Align outperforms the baselines in terms of background preservation, especially for the Bison and Imagen datasets which have more elaborate captions than Dream.

		FID↓	LPIPS↓	PWMSE↓
Dream	FlexIT	154.44 ± 0.19	0.31 ± 0.00	30.22 ± 0.05
	InstructPix2Pix	147.62 ± 0.82	0.25 ± 0.00	27.87 ± 0.35
	ControlNet	137.29 ± 1.86	0.31 ± 0.00	32.74 ± 0.42
	DiffEdit	125.95 ± 0.44	0.15 ± 0.00	15.72 ± 0.04
	Plug-and-Play	151.42 ± 1.02	0.34 ± 0.00	31.59 ± 0.00
	Imagic	174.41 ± 1.49	0.42 ± 0.00	31.63 ± 0.08
	DM-Align	102.44 ± 0.07	0.11 ± 0.00	14.54 ± 0.01
Bison	FlexIT	35.48 ± 0.07	0.24 ± 0.00	20.38 ± 0.03
	InstructPix2Pix	44.01 ± 0.28	0.26 ± 0.00	20.00 ± 0.06
	ControlNet	35.39 ± 0.06	0.25 ± 0.00	26.58 ± 0.04
	DiffEdit	37.68 ± 0.33	0.23 ± 0.00	19.68 ± 0.09
	Plug-and-Play	36.44 ± 0.78	0.24 ± 0.00	19.79 ± 0.12
	Imagic	43.55 ± 0.76	0.27 ± 0.00	27.12 ± 0.10
	DM-Align	16.41 ± 0.00	0.08 ± 0.00	14.16 ± 0.00
Imagen	FlexIT	92.44 ± 0.35	0.36 ± 0.00	36.57 ± 0.01
	InstructPix2Pix	124.32 ± 0.80	0.46 ± 0.00	34.29 ± 0.15
	ControlNet	85.56 ± 0.31	0.42 ± 0.00	49.78 ± 0.02
	DiffEdit	88.01 ± 0.55	0.31 ± 0.00	24.17 ± 0.09
	Plug-and-Play	81.28 ± 0.28	0.34 ± 0.00	31.59 ± 0.07
	Imagic	103.74 ± 1.49	0.56 ± 0.00	43.91 ± 0.08
	DM-Align	54.12 ± 0.04	0.21 ± 0.00	22.09 ± 0.00

Table 4: Ablation tests for the Imagen dataset (mean and variance). The results underscore the significance of all DM-Align components. "Non-shared objects" denote objects mentioned solely in the source caption, while "Refinement of diffusion mask" involves adjusting the diffusion mask through shrinkage or expansion based on regions corresponding to keywords.

	FID↓	LPIPS↓	PWMSE↓	CLIPScore↑
(w/o) diffusion mask	43.36 ± 1.44	0.42 ± 0.00	41.61 ± 0.26	0.77 ± 0.00
(w/o) noise cancellation	44.44 ± 0.76	0.41 ± 0.00	40.57 ± 0.30	0.79 ± 0.00
(w/o) refinement of diffusion mask	47.63 ± 0.78	0.43 ± 0.00	43.60 ± 0.15	0.77 ± 0.00
(w/o) objects with different modifiers	42.34 ± 0.57	0.40 ± 0.00	38.23 ± 0.20	0.77 ± 0.00
(w/o) non-shared objects	45.35 ± 2.25	0.43 ± 0.00	41.57 ± 0.79	0.77 ± 0.00
DM-Align	40.05 ± 0.00	0.39 ± 0.00	37.05 ± 0.00	0.78 ± 0.00

datasets devoid of source text descriptions, FlexIT and DiffEdit are evaluated on a subset of the ImageNet dataset (Deng et al., 2009), which assumes the replacement of the main object of the image with another object. Additionally, DiffEdit is evaluated on the Bison dataset (Hu et al., 2019) and a self-defined collection of Imagen pictures (Saharia et al., 2022). Out of these datasets, our model is evaluated using the Bison dataset and the collection of images generated by Imagen (further referred to as the Imagen dataset) described by Couairon et al. (2023). We omit the ImageNet dataset due to its oversimplified setup, primarily employing single-word source and target text instructions.

Bison and Imagen datasets contain elaborated text captions with up to 23 words. To investigate the behavior of the DM-Align model and the baseline models when confronted with shorter text in-

structions we generate a collection of 100 images using Dream by WOMBO² that relies on the source captions as guidance. As the dataset is generated using Dream by Wombo, we further refer to it as Dream. To complete the Dream dataset, we specify a new text query as the target instruction for each image-instruction pair. Unlike the Imagen and Bison datasets, the text instructions of Dream do not contain more than 11 words.

Evaluation metrics.

To evaluate our model, we use a set of metrics that assess the similarity of the edited image to both the input image and the target instruction. By default, it is a trade-off between image-based and text-based metrics as we need to find the best equilibrium point.

²The code is available at <https://github.com/cdgco/dream-api>

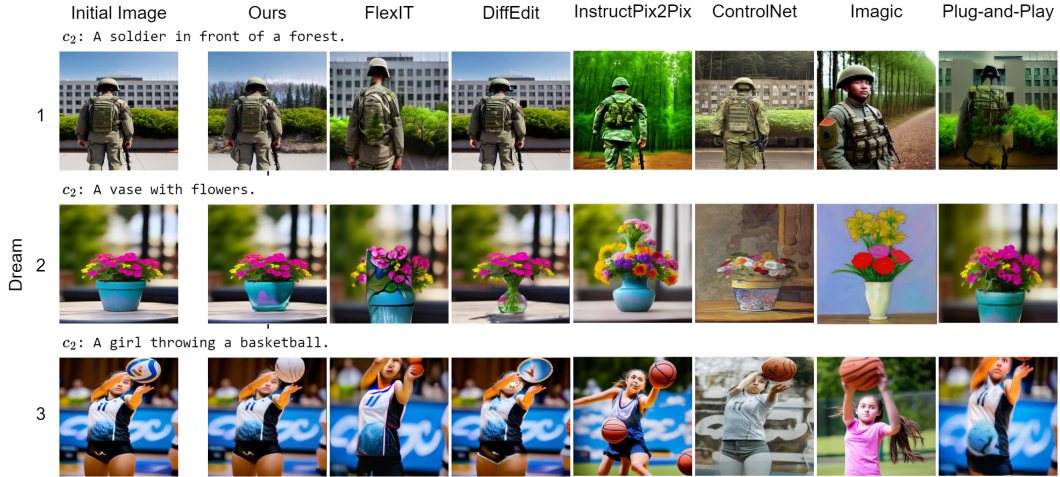


Figure 6: Semantic image editing: Dream dataset. Source captions: (1) c_1 . A soldier in front of a building. (2) c_1 . A pot with flowers. (3) c_1 . A girl throwing a volleyball.

Generating images close to the source image improves the image-based metrics while reducing the similarity to the target caption. On the other hand, images close to the target instruction improve the text-based scores but can affect the similarity to the input picture. The equilibrium point is important given that people tend to focus mainly on specifying the desired changes in an image while omitting the information that already exists (Hurley, 2014). Therefore, the edited content can represent a small region of the new image while the rest of it should keep the content of the source image.

The similarity (or the distance) of the updated image w.r.t the source image is assessed using FID (Heusel et al., 2017), LPIPS (Zhang et al., 2018) and the pixel-wise Mean Square Error (PWMSE). FID relies on the difference between the distributions of the last layer of the Inception V3 model (Szegedy et al., 2016) that separately runs over the input and edited images. FID measures the consistency and image realism of the new image w.r.t the source image. Contrary to the quality assessment computed by FID, LPIPS measures the perceptual similarity by calculating the distance between layers of an arbitrary neural network that separately runs over the input and updated images. As the LPIPS metric, PWMSE determines the pixel leakage by computing the pixel-wise error between the input and the edited images. The similarity of the updated image w.r.t the target instruction is computed in the CLIP multimodal embedding space by the CLIPScore (Hessel et al., 2021). More details about the evaluation metrics are specified in Appendix B.

5 Results and discussion

5.1 Quantitative analysis and ablation tests

How well can the DM-Align model edit a source image considering the length of the text instruction? To address the first research question, we refer to Table 1. When compared to the baselines Diffedit, ControlNet, FlexIT, Plug-and-Play, and InstructPix2Pix, our proposed DM-Align model exhibits particularly effective performance in terms of image-based metrics.

This effectiveness is particularly noticeable in the Bison and Imagen datasets, which contain longer captions compared to the Dream dataset. When compared with the best baseline over the Imagen dataset, DM-Align improves FID, LPIPS, and PWMSE by 23.42%, 19.87%, and 3.32%, respectively. Similar results are observed for the Bison dataset, where DM-Align enhances the results of the best baseline by 4.22% for FID, by 14.26% for LPIPS, and by 11.20% for PWMSE. In the case of the Dream dataset, DM-Align still outperforms other baselines in terms of FID and PWMSE, albeit with smaller margins. However, in terms of LPIPS, DiffEdit outperforms DM-Align over the instance of the Dream dataset.

Given the results presented in Table 1, we posit that baselines find it easier to accurately edit images using short text instructions. Conversely, when text instructions are more elaborate, such as in the Bison and Imagen datasets, results significantly surpass those achieved by the baselines. DM-Align leverages word alignments between source and target instructions, highlighting their crucial role in

facilitating effective image editing.

In terms of text-based metrics, CLIPScore suggests that FlexIT generates images closest to the target instructions. This outcome is likely attributed to FlexIT’s architecture, which is based on a CLIP model—the same model used to calculate CLIPScore. This issue is highlighted in (Poole et al., 2023). Another possible explanation is that FlexIT is trained to maximize the similarity between input images and instructions. As depicted in Figures 3, 5, and 6, FlexIT may sacrifice image quality for higher similarity scores. Regarding CLIPScore, DM-Align consistently outperforms Plug-and-Play, Imagic and DiffEdit baselines or is equally effective as InstructPix2Pix and ControlNet. DM-Align also outperforms Prompt-to-Prompt (Hertz et al., 2023). As Prompt-to-Prompt can edit only self-generated images the comparison with DM-Align is limited only to text-based metrics like CLIPScore. More details about this comparison are presented in Appendix C.

Given the text-based and image-based metrics, DM-Align seems to properly preserve the content of the input image and obtain a better trade-off between closeness to the input picture and target instruction than the baselines.

While the above analysis demonstrates that elaborate text instructions do not affect the editing capabilities of DM-Align, unlike the baselines, we are also interested in examining how the degree of overlap between source and target captions impacts the quality of the edited image. To analyze this, we select 575 Bison instances with a similarity between the source and target instructions higher than Rouge 0.75. We do not conduct this analysis for the Imagen and Dream datasets as their text instructions already exhibit a level of similarity higher than Rouge 0.75. Our analysis is limited to DM-Align, FlexIT, and DiffEdit, as the other baselines do not utilize source captions in their implementation and are therefore omitted from this analysis. The results are presented in Table 2. We observe that while the results are similar to the image-based and text-based scores reported in Table 1 for Bison, all models report better performance and an improved trade-off between image and text-based metrics. These results suggest that increased overlap between source and target captions enhances the quality of image editing.

How well does the DM-Align model preserve the background? To extract the background, we con-

sider the DM-Align mask obtained after adjusting the diffusion mask. Upon analyzing the results presented in Table 3, the first notable observation is the significant reduction in the FID score of the DM-Align model by 73.27% for the Bison dataset, 40.12% for the Imagen dataset, and 20.58% for the Dream dataset when compared with the best baseline. Similarly, the LPIPS and PWMSE scores also indicate significant margin reductions, particularly for the Bison and Imagen datasets. Concerning the Dream dataset, DM-Align still outperforms the best-performing baseline with a margin of 25.02% for LPIPS and 7.80% for PWMSE. While DM-Align consistently demonstrates superior results for background preservation, we infer that the baselines are relatively adept at preserving the background only when the instructions are short and simple, as observed in the case of the Dream dataset. This conclusion is further supported by the results presented in Table 1.

Ablation tests To run the ablation tests for DM-Align we rely on the Imagen dataset. According to Table 4, the absence of the refinement of the diffusion mask using the regions detected with the word alignment model and the Grounding-SAM segmentation model has the highest negative impact over the similarity w.r.t the input picture. As expected, a significant negative effect over the similarity with the input image is also noticed when omitting the deleted nouns or the nouns with different modifiers in the two queries. Similarly, noise cancellation and especially the diffusion mask also affect the conservation of the background. Including all the components in the architecture of DM-Align mainly facilitates the preservation of the input image and does not result in a reduction of the CLIPScore. Therefore, the inclusion of all these components in the DM-Align represents the best trade-off w.r.t the similarity to the input image and to the target caption.

The next five visualizations exemplify the ablation tests. The first row of each figure presents the effect of omitting a component of DM-Align, while the correct behavior is shown in the second row. Figure 7 illustrates the effect of defining the editing mask based only on the image regions of the keywords. Without the diffusion mask, the model has to insert a new object in the fixed area of the replaced object. If we need to replace an object with a larger one, DM-Align without diffusion might create distorted and unnatural outputs. As we usu-



Figure 7: 1st line: Example of omitting the diffusion mask (c_1 : A woman near a cat., c_2 : A woman near a dog.). 2nd line: The correct example of including the diffusion mask.



Figure 8: 1st line: Example of omitting the cancellation of the noise variable defined within the diffusion model. (c_1 : A man sitting at a table holding a laptop on the train., c_2 : A man sitting at a table reading a book on the train.). 2nd line: The correct example of including the noise cancellation.

ally expect bigger dogs than cats, DM-Align with diffusion properly replaces the cat with a slightly bigger dog. On the contrary, the dog that replaced the cat is distorted when diffusion is not used.

While the overall diffusion mask can give more context for the editing and allows the insertion of objects of different sizes, noise cancellation is an important step used to improve the initial diffusion mask. As shown in Figure 8, when noise cancellation is used, the initial diffusion mask is better trimmed, and the background is properly preserved.

As the diffusion mask does not have complete control over the regions to be edited, its extension or shrinkage based on the image regions of the keywords is mandatory to obtain a correct mask for editing. When the image is edited using only the initial diffusion mask in Figure 9, both the ship and the sand are modified, while the former is expected to be preserved. As opposed, when the diffusion mask is refined with image segmentation, only the sand is replaced by the ocean.

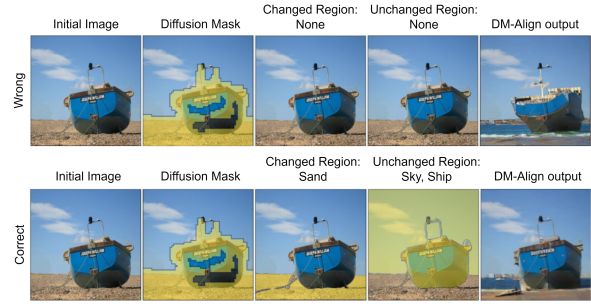


Figure 9: 1st line: Example of omitting the refinement of the diffusion mask using image segmentation (c_1 : A clear sky and a ship landed on the sand., c_2 : A clear sky and a ship landed on the ocean.). 2nd line: The correct example of including the refinement of the diffusion mask with image segmentation.



Figure 10: 1st line: Example of omitting the information about modifiers associated with the nouns shared by both captions (c_1 : A woman with a red jacket., c_2 : A woman with a green jacket.). 2nd line: The correct example of including the information about the modifiers.

The omission of the adjective modifiers in the analysis of DM-Align is exemplified in Figure 10. If the modifiers are left out, DM-Align considers the jacket a shared noun, like the noun “woman”, and removes its regions from the diffusion mask. As a result, DM-Align does not detect any semantical difference between the text instructions, and the output image is identical to the input image. On the other hand, if the modifiers are considered, DM-Align can properly adjust the color of the jacket while keeping the woman’s face unaltered.

As we are interested to make only the necessary updates in the picture, while keeping the background and the regions of the deleted words unchanged, the region assigned to the word “man” in Figure 11 is removed from the diffusion mask. As a result, the corresponding region is untouched. On the contrary, the inclusion of the region associated with the word “man” in the diffusion mask increases the randomness in the new image by inserting a store. Since the store is irrelevant, both

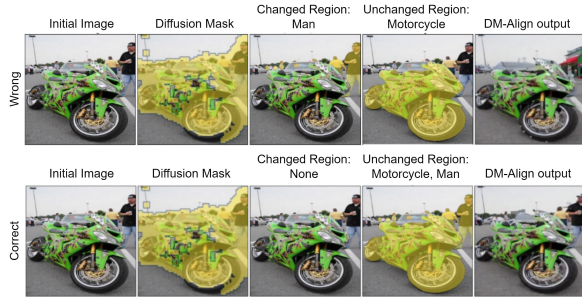


Figure 11: 1st line: Example of omitting the information about the deleted nouns from the source caption (c_1 : A motorcycle near a man., c_2 : A motorcycle.). 2nd line: The correct example of including the information about the deleted nouns.

the similarity scores w.r.t the input image or target instruction are reduced.

5.2 Human qualitative analysis

Some qualitative examples extracted from the three data collections are shown in Figures 3, 5, and 6. Compared to DIFFEEdit, ControlNet, and FlexIT, as well as Plug-and-Play, Imagic and InstructPix2Pix, the DM-Align model demonstrates superior manipulation of the content of the input image while largely preserving the background in line with the target query. DM-Align establishes semantic connections between source and target queries, updating the image content accordingly, whereas the baselines often alter the background more than necessary, as discussed above. DiffEdit tends to introduce random visual content (see Figure 3), while FlexIT tends to distort and zoom into the image (Figures 5 and 6), trading off the minimization of the reconstruction loss with respect to the input image and the text instructions for potential distortions in the new image. Although ControlNet can maintain the structure of the input image, it struggles to preserve the texture or colors of the objects, likely due to the absence of a masking system. InstructPix2Pix also encounters challenges in preserving the style of objects in the input image and tends to include more objects in the image than specified in the target text instruction. Plug-and-Play zooms into the image and tends to slightly alter the details of objects requested for preservation in the target text instruction. Out of all baselines, Imagic shows the highest tendency to change the input image’s compositional structure, as highlighted also by the image-based metrics presented in Tables 1 and 3.

Table 5: Human evaluation of the quality of the editing process based on the text instruction (Q1), the preservation of the background (Q2) and the quality of the edited image (Q3). The results represent the average scores reported by annotators using a 5-point Likert scale.

	Q1↑	Q2↑	Q3↑
FlexIt	3.75	4.00	3.85
DiffEdit	3.85	4.15	3.85
ControlNet	3.50	3.75	3.90
Plug-and-Play	3.80	4.10	3.85
InstructPix2Pix	3.50	3.75	3.80
Imagic	3.80	3.20	3.85
DM-Align	3.90	4.35	3.95

To confirm the above observations, we randomly selected 100 images from the Bison dataset and asked Amazon MTurk annotators to evaluate the editing quality of the five baselines and the proposed DM-Align. For each edited image, the annotators were asked to evaluate the overall quality of the editing process based on the text instruction (Q1), the preservation of the background (Q2) and the quality of the edited image in terms of compositionality, sharpness, distortion, color and contrast (Q3). According to the human evaluation executed on a 5-point Likert scale, our model scores better than all baselines (Table 5). The inter-rater agreement is good with Cohen’s weighted kappa κ between 0.65 and 0.75 for all analyzed models.

6 Conclusion, limitations and future work

We propose a novel model DM-Align for semantic image editing that confers to the users a natural control over the image editing by updating the text instructions. By automatically identifying the regions to be kept or altered purely based on the text instructions, the proposed model is not a black box. Due to the high level of explainability, the users can easily understand the edited result and how to change the instructions to obtain the desired output.

The quantitative and qualitative evaluations show the superiority of DM-Align to enhance the text-based control of semantic image editing over existing baselines FlexIT, DiffEdit, ControlNet, Imagic, Plug-and-Play and InstructPix2Pix. Unlike the latter models, our approach is not limited by the length of the text instructions. Due to the inclusion of one-to-one alignments between the words of the instructions that describe the image before and after the image update, we can edit images regardless of how complicated and elaborate the text instructions are. Besides the low sensitivity to the complexity of the instructions, the one-to-one word alignments

allow us to properly conserve the background while editing only what is strictly required by the users.

DM-Align focuses on the editing of objects mentioned as nouns and their adjectives. In future work, its flexibility can be improved by editing actions in which objects and persons are involved. As a result, they might change position in the image without the need to update their properties.

Acknowledgments

This project was funded by the European Research Council (ERC) Advanced Grant CALCULUS (grant agreement No. 788506).

References

- Omri Avrahami, Ohad Fried, and Dani Lischinski. 2023. Blended latent diffusion. *ACM Trans. Graph.*, 42(4):149:1–149:11.
- Omri Avrahami, Dani Lischinski, and Ohad Fried. 2022. Blended diffusion for text-driven editing of natural images. In *2022 Conference on Computer Vision and Pattern Recognition (CVPR 2022)*, pages 18187–18197. IEEE.
- Tim Brooks, Aleksander Holynski, and Alexei A. Efros. 2023. Instructpix2pix: Learning to follow image editing instructions. In *2023 Conference on Computer Vision and Pattern Recognition (CVPR 2023)*, pages 18392–18402. IEEE.
- P.W.D. Charles. 2023. Grounded-sam. <https://github.com/IDEA-Research/Grounded-Segment-Anything/tree/main>.
- Jooyoung Choi, Sungwon Kim, Yonghyun Jeong, Youngjune Gwon, and Sungroh Yoon. 2021. ILVR: conditioning method for denoising diffusion probabilistic models. In *2021 International Conference on Computer Vision (ICCV 2021)*, pages 14347–14356. IEEE.
- Guillaume Couairon, Asya Grechka, Jakob Verbeek, Holger Schwenk, and Matthieu Cord. 2022. Flexit: Towards flexible semantic image translation. In *2022 Conference on Computer Vision and Pattern Recognition (CVPR 2022)*, pages 18270–18279. IEEE.
- Guillaume Couairon, Jakob Verbeek, Holger Schwenk, and Matthieu Cord. 2023. Diffedit: Diffusion-based semantic image editing with mask guidance. In *11th International Conference on Learning Representations (ICLR 2023)*. OpenReview.net.
- Jia Deng, Wei Dong, Richard Socher, Li-Jia Li, Kai Li, and Li Fei-Fei. 2009. Imagenet: A large-scale hierarchical image database. In *2009 Computer Society Conference on Computer Vision and Pattern Recognition (CVPR 2009)*, pages 248–255. IEEE.
- Ming Ding, Zhuoyi Yang, Wenyi Hong, Wendi Zheng, Chang Zhou, Da Yin, Junyang Lin, Xu Zou, Zhou Shao, Hongxia Yang, and Jie Tang. 2021. Cogview: Mastering text-to-image generation via transformers. In *35th Annual Conference on Neural Information Processing Systems (NeurIPS 2021)*, pages 19822–19835.
- Ming Ding, Wendi Zheng, Wenyi Hong, and Jie Tang. 2022. Cogview2: Faster and better text-to-image generation via hierarchical transformers. In *36th Annual Conference on Neural Information Processing Systems 2022 (NeurIPS 2022)*.
- Ian J. Goodfellow, Jean Pouget-Abadie, Mehdi Mirza, Bing Xu, David Warde-Farley, Sherjil Ozair, Aaron C. Courville, and Yoshua Bengio. 2014. Generative adversarial nets. In *31st Conference on Neural Information Processing Systems (NeurIPS 2014)*, pages 2672–2680.
- Kaiming He, Xiangyu Zhang, Shaoqing Ren, and Jian Sun. 2015. Delving deep into rectifiers: Surpassing human-level performance on imagenet classification. In *2015 International Conference on Computer Vision (ICCV 2015)*, pages 1026–1034.
- Amir Hertz, Ron Mokady, Jay Tenenbaum, Kfir Aberman, Yael Pritch, and Daniel Cohen-Or. 2023. Prompt-to-prompt image editing with cross-attention control. In *11th International Conference on Learning Representations (ICLR 2023)*. OpenReview.net.
- Jack Hessel, Ari Holtzman, Maxwell Forbes, Ronan Le Bras, and Yejin Choi. 2021. Clipscore: A reference-free evaluation metric for image captioning. In *2021 Conference on Empirical Methods in Natural Language Processing (EMNLP 2021)*, pages 7514–7528. ACL.
- Martin Heusel, Hubert Ramsauer, Thomas Unterthiner, Bernhard Nessler, and Sepp Hochreiter. 2017. Gans trained by a two time-scale update rule converge to a local nash equilibrium. In *31st Conference on Neural Information Processing Systems (NeurIPS 2017)*, pages 6626–6637.
- Jonathan Ho, Ajay Jain, and Pieter Abbeel. 2020. Denoising diffusion probabilistic models. In *34th Annual Conference on Neural Information Processing Systems 2020 (NeurIPS 2020)*.
- Hexiang Hu, Ishan Misra, and Laurens van der Maaten. 2019. Evaluating text-to-image matching using binary image selection (BISON). In *2019 International Conference on Computer Vision Workshops (ICCV 2019)*, pages 1887–1890. IEEE.
- Patrick J Hurley. 2014. *A concise introduction to logic*. Cengage Learning.
- Mandar Joshi, Danqi Chen, Yinhan Liu, Daniel S. Weld, Luke Zettlemoyer, and Omer Levy. 2020. SpanBERT: Improving pre-training by representing and predicting spans. *Transactions of the Association for Computational Linguistics*, 8.

- Jared Kaplan, Sam McCandlish, Tom Henighan, Tom B. Brown, Benjamin Chess, Rewon Child, Scott Gray, Alec Radford, Jeffrey Wu, and Dario Amodei. 2020. Scaling laws for neural language models. *arXiv preprint arXiv:2001.08361*.
- Bahjat Kawar, Shiran Zada, Oran Lang, Omer Tov, Huiwen Chang, Tali Dekel, Inbar Mosseri, and Michal Irani. 2023. Imagic: Text-based real image editing with diffusion models. In *2023 Conference on Computer Vision and Pattern Recognition (CVPR 2023)*, pages 6007–6017. IEEE.
- Diederik P. Kingma and Max Welling. 2014. Auto-encoding variational bayes. In *2nd International Conference on Learning Representations (ICLR 2014)*.
- Alexander Kirillov, Eric Mintun, Nikhila Ravi, Hanzi Mao, Chloé Rolland, Laura Gustafson, Tete Xiao, Spencer Whitehead, Alexander C. Berg, Wan-Yen Lo, Piotr Dollár, and Ross B. Girshick. 2023. Segment anything. In *2023 International Conference on Computer Vision (ICCV 2023)*, pages 3992–4003. IEEE.
- Wuwei Lan, Chao Jiang, and Wei Xu. 2021. Neural semi-markov CRF for monolingual word alignment. In *59th Annual Meeting of the Association for Computational Linguistics and the 11th International Joint Conference on Natural Language Processing (ACL/IJCNLP 2021)*, pages 6815–6828. ACL.
- Bowen Li, Xiaojuan Qi, Thomas Lukasiewicz, and Philip H. S. Torr. 2020. Manigan: Text-guided image manipulation. In *2020 Conference on Computer Vision and Pattern Recognition (CVPR 2020)*, pages 7877–7886. Computer Vision Foundation / IEEE.
- Shilong Liu, Zhaoyang Zeng, Tianhe Ren, Feng Li, Hao Zhang, Jie Yang, Chunyuan Li, Jianwei Yang, Hang Su, Jun Zhu, and Lei Zhang. 2023. [Grounding DINO: marrying DINO with grounded pre-training for open-set object detection](#). *CoRR*, abs/2303.05499.
- Ben Poole, Ajay Jain, Jonathan T. Barron, and Ben Mildenhall. 2023. Dreamfusion: Text-to-3d using 2d diffusion. In *11th International Conference on Learning Representations (ICLR 2023)*. OpenReview.net.
- Aditya Ramesh, Prafulla Dhariwal, Alex Nichol, Casey Chu, and Mark Chen. 2022. Hierarchical text-conditional image generation with CLIP latents. *arXiv preprint arXiv:2204.06125*.
- Aditya Ramesh, Mikhail Pavlov, Gabriel Goh, Scott Gray, Chelsea Voss, Alec Radford, Mark Chen, and Ilya Sutskever. Zero-shot text-to-image generation. In *38th International Conference on Machine Learning (ICML 2021)*, volume 139 of *Proceedings of Machine Learning Research*, pages 8821–8831. PMLR.
- Scott E. Reed, Zeynep Akata, Xinchun Yan, Lajanugen Logeswaran, Bernt Schiele, and Honglak Lee. 2016. Generative adversarial text to image synthesis. In *3rd International Conference on Machine Learning, (ICML 2016)*, volume 48 of *JMLR Workshop and Conference Proceedings*, pages 1060–1069. JMLR.org.
- Robin Rombach, Andreas Blattmann, Dominik Lorenz, Patrick Esser, and Björn Ommer. 2022. High-resolution image synthesis with latent diffusion models. In *2022 Conference on Computer Vision and Pattern Recognition (CVPR 2022)*, pages 10674–10685. IEEE.
- Chitwan Saharia, William Chan, Saurabh Saxena, Lala Li, Jay Whang, Emily L. Denton, Seyed Kammar Seyed Ghasemipour, Raphael Gontijo Lopes, Burcu Karagol Ayan, Tim Salimans, Jonathan Ho, David J. Fleet, and Mohammad Norouzi. 2022. Photorealistic text-to-image diffusion models with deep language understanding. In *36th Annual Conference on Neural Information Processing Systems (NeurIPS 2022)*.
- Uriel Singer, Adam Polyak, Thomas Hayes, Xi Yin, Jie An, Songyang Zhang, Qiyuan Hu, Harry Yang, Oron Ashual, Oran Gafni, Devi Parikh, Sonal Gupta, and Yaniv Taigman. 2023. Make-a-video: Text-to-video generation without text-video data. In *11th International Conference on Learning Representations (ICLR 2023)*. OpenReview.net.
- Christian Szegedy, Vincent Vanhoucke, Sergey Ioffe, Jonathon Shlens, and Zbigniew Wojna. 2016. Re-thinking the inception architecture for computer vision. In *2016 Conference on Computer Vision and Pattern Recognition (CVPR 2016)*, pages 2818–2826. IEEE Computer Society.
- Kristina Toutanova, Dan Klein, Christopher D. Manning, and Yoram Singer. 2003. Feature-rich part-of-speech tagging with a cyclic dependency network. In *Human Language Technology Conference of the North American Chapter of the Association for Computational Linguistics (HLT-NAACL 2003)*. The Association for Computational Linguistics.
- Narek Tumanyan, Michal Geyer, Shai Bagon, and Tali Dekel. 2023. Plug-and-play diffusion features for text-driven image-to-image translation. In *2023 Conference on Computer Vision and Pattern Recognition CVPR 2023*, pages 1921–1930. IEEE.
- Ashish Vaswani, Noam Shazeer, Niki Parmar, Jakob Uszkoreit, Llion Jones, Aidan N. Gomez, Lukasz Kaiser, and Illia Polosukhin. 2017. Attention is all you need. In *31st Conference on Neural Information Processing Systems (NeurIPS 2017)*, pages 5998–6008.
- Su Wang, Chitwan Saharia, Ceslee Montgomery, Jordi Pont-Tuset, Shai Noy, Stefano Pellegrini, Yasumasa Onoe, Sarah Laszlo, David J. Fleet, Radu Soricut, Jason Baldridge, Mohammad Norouzi, Peter Anderson, and William Chan. 2023. Imagen editor and editbench: Advancing and evaluating text-guided image inpainting. In *2023 Conference on Computer Vision and Pattern Recognition (CVPR 2023)*, pages 18359–18369. IEEE.

Lilian Weng. 2021. What are diffusion models? *lilian-weng.github.io*.

Shaoan Xie, Zhifei Zhang, Zhe Lin, Tobias Hinz, and Kun Zhang. 2023. Smartbrush: Text and shape guided object inpainting with diffusion model. In *2023 Conference on Computer Vision and Pattern Recognition (CVPR 2023)*, pages 22428–22437. IEEE.

Xuchen Yao. 2014. *Feature-driven question answering with natural language alignment*. Ph.D. thesis, Johns Hopkins University.

Lvmin Zhang, Anyi Rao, and Maneesh Agrawala. 2023a. Adding conditional control to text-to-image diffusion models. In *2023 International Conference on Computer Vision (ICCV 2023)*, pages 3813–3824. IEEE.

Richard Zhang, Phillip Isola, Alexei A. Efros, Eli Shechtman, and Oliver Wang. 2018. The unreasonable effectiveness of deep features as a perceptual metric. In *2018 Conference on Computer Vision and Pattern Recognition (CVPR 2018)*, pages 586–595. IEEE Computer Society.

Zicheng Zhang, Bonan Li, Xuecheng Nie, Congying Han, Tiande Guo, and Luoqi Liu. 2023b. Towards consistent video editing with text-to-image diffusion models. In *37th Annual Conference on Neural Information Processing Systems (NeurIPS 2023)*.

Minfeng Zhu, Pingbo Pan, Wei Chen, and Yi Yang. 2019. DM-GAN: dynamic memory generative adversarial networks for text-to-image synthesis. In *2019 Conference on Computer Vision and Pattern Recognition (CVPR 2019)*, pages 5802–5810. Computer Vision Foundation / IEEE.

Appendix

A. Implementation Details

We use Stable Diffusion v1.4 with 50 diffusion steps and a guidance scale of 7.5 to run DM-Align. The size of the generated images is 512×512 pixels. For consistency reasons, we use Stable Diffusion v1.4 to run DiffEdit, ControlNet, Plug-and-Play and Imagic. In the case of InstructPix2Pix, we use the Stable Diffusion model fine-tuned by the authors. Following the implementation details mentioned in their papers, ControlNet, Plug-and-Play, DiffEdit, Imagic and InstructPix2Pix edit images at a resolution of 512×512 pixels. DiffEdit, ControlNet, Imagic and Plug-and-Play require 50 diffusion steps, while InstructPix2Pix manipulates images using 100 diffusion steps. The resolution of images edited by FlexIT is 288×288 pixels, according to

the indication in its paper. All experiments are implemented using one NVIDIA GeForce RTX 3080 GPU.

B. Evaluation Metrics

Image-based evaluation metrics:

- The FID score relies on the distribution of the output generated by the last layer of the Inception V3 model (Szegedy et al. 2016). The metric is computed by measuring the Frechet distance between the distributions gleaned by running the Inception V3 model over the source and target images. Considering the mean μ_1 and the covariance C_1 of the source images and the mean μ_2 and the covariance C_2 of the target images, the FID score is computed as follows:

$$FID = \|\mu_1 - \mu_2\|_2^2 + \text{Tr}(C_1 + C_2 - 2(C_1 C_2)^{1/2}) \quad (6)$$

- LPIPS measures the average Euclidean distance between outputs of different layers of a neural network (AlexNet for the current study, as suggested by Zhang et al. (2018)) obtained by giving as input the source and the target images. Considering $x_1^l, \hat{x}_2^l \in \mathcal{R}^{H_l \times W_l \times C_l}$ as the intermediate l -th representations of the AlexNet for the source and the predicted target image, respectively, the LPIPS score is defined by:

$$LPIPS = \sum_l \frac{1}{H_l W_l} \sum_{h,w} |x_{1hw}^l - (\hat{x}_2)_{hw}^l|^2 \quad (7)$$

- PWMSE measures the pixel-wise mean square error between the input and the edited image.

Text-based evaluation metrics:

- CLIPScore measures the cosine similarity between the CLIP text embedding c_{clip} and CLIP image embedding v_{clip} . The metric is computed as $2.5 * \max(\cos(c_{clip}, v_{clip}), 0)$. Following the indication of Hessel et al. (2021), CLIP latent embedding space is computed using a Vision Transformer for image encoding and a Transformer for text encoding.

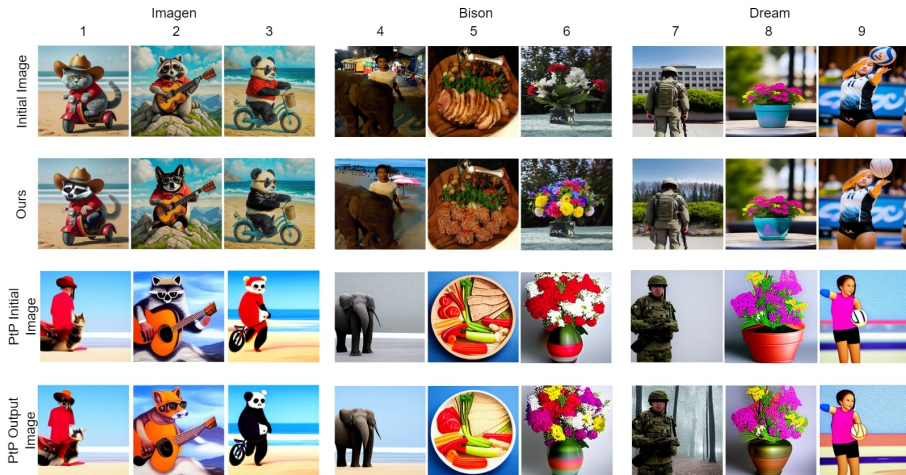


Figure 12: Semantic image editing: Comparison between Prompt-to-Prompt (PtP) and DM-Align. Source captions: (1) c_1 . A photo of a British shorthair cat wearing a cowboy hat and red shirt riding a bike on a beach. c_2 . A photo of a raccoon wearing a cowboy hat and red shirt riding a bike on a beach. (2) c_1 . An oil painting of a raccoon wearing sunglasses and red shirt playing a guitar on top of a mountain. c_2 . An oil painting of a Shiba Inu dog wearing sunglasses and red shirt playing a guitar on top of a mountain. (3) c_1 . An oil painting of a fuzzy panda wearing sunglasses and red shirt riding a bike on a beach. c_2 . An oil painting of a fuzzy panda wearing sunglasses and black jacket riding a bike on a beach. (4) c_1 . A man standing next to a baby elephant in the city. c_2 . A man standing next to his elephant on the beach. (5) c_1 . A wooden plate topped with sliced meat and vegetables. c_2 . A plate of rice meat and vegetables. (6) c_1 . A vase filled with red and white flowers. c_2 . A vase filled with lots of colorful flowers. (7) c_1 . A soldier in front of a building. c_2 . A soldier in front of a forest. (8) c_1 . A pot with flowers. c_2 . A vase with flowers. (9) c_1 . A girl throwing a volleyball. c_2 . A girl throwing a basketball.

Table 6: Image-level evaluation of DM-Align with Stable diffusion and Blended latent diffusion for inpainting. The results are reported for the Dream dataset (mean and variance).

	FID↓	LPIPS↓	PWMSE↓	CLIPScore↑
DM-Align (Blended Latent Diffusion)	128.87 ± 0.12	0.33 ± 0.00	32.50 ± 0.43	0.78 ± 0.00
DM-Align (Statble Latent Diffusion)	124.57 ± 0.52	0.31 ± 0.00	29.24 ± 0.03	0.80 ± 0.00

Table 7: Image-level evaluation (mean and variance) of DM-Align and Prompt-to-Prompt using Dream and Imagen datasets.

	CLIPScore↑ (Dream)	CLIPScore↑ (Imagen)
Prompt-to-Prompt	0.76 ± 0.00	0.75 ± 0.00
DM-Align	0.80 ± 0.00	0.78 ± 0.00

C. Additional results

Table 6 presents the results of the comparison between Stable Diffusion and Blended Latent Diffusion for editing the masked regions detected by DM-Align. According to all image-based and text-based metrics, Stable Diffusion confers more robust editing capabilities than Blended Latent Diffusion and it is therefore used to implement DM-Align.

The comparison between DM-Align and Prompt-to-Prompt is presented in Table 7. Since Prompt-

to-Prompt cannot edit real images but only images generated using the source text instruction, the comparison is limited to CLIPScore. Based on the provided results, the images edited by DM-Align better align with the target text instructions than those edited by Prompt-to-Prompt. The discrepancy in CLIPScore between DM-Align and Prompt-to-Prompt may also be attributed to the fact that the initial images generated by Prompt-to-Prompt do not always reflect the entire source text instructions (images 1 and 4 in Figure 12). Regarding the similarity with the input images generated using the source caption, Prompt-to-Prompt encounters difficulties in preserving the background, as one can see in images 6, 8, and 9 of Figure 12.